IEEE Access
Multidisciplinary | Rapid Review | Open Access Journal

Received December 13, 2019, accepted December 27, 2019, date of publication January 13, 2020, date of current version January 24, 2020.

Digital Object Identifier 10.1109/ACCESS.2020.2966004

Research on Sinusoidal Error Compensation of Moiré Signal Using Particle Swarm Optimization

WEIBIN ZHU[1], YU LIN[1], YAO HUANG[2,3], AND ZI XUE[3]
[1]College of Measurement and Testing Engineering, China Jiliang University, Hangzhou 310018, China
[2]College of Optical Science and Engineering, Zhejiang University, Hangzhou 310027, China
[3]National Institute of Metrology, Beijing 100029, China

Corresponding author: Weibin Zhu (zhuweibin@cjlu.edu.cn)

This work was supported in part by the project of the National Key Research and Development Program of China under Grant 2017YFF0204901, and in part by the Research Project of General Administration of Quality Supervision, Inspection and Quarantine of PRC under Grant 2016QK189.

ABSTRACT In this paper, the sinusoidal error compensation method based on particle swarm optimization (PSO) is researched to reduce the subdivision precision loss caused by sinusoidal error in a grating moiré signal. On the basis of the principle of arctangent subdivision of a grating moiré signal, the subdivision error caused by sinusoidal error is quantitatively analysed. In view of the sinusoidal error compensation method, the signal compensation method involves complex calculations and occupies many resources; therefore, a sinusoidal error angle compensation method is proposed. The principle of the sinusoidal error angle compensation method based on the PSO algorithm is explained in detail. Aiming at the large calculation amount of the PSO algorithm, the appropriate PSO parameters are selected experimentally, and the complexity of the PSO algorithm is minimized while ensuring the fitting accuracy. The parameters of the signal waveform equation are solved using the PSO algorithm on the field-programmable gate array (FPGA) platform. According to the parameters solved, a lookup table for sinusoidal error compensation is designed. The grating system platform is built to verify the effect of the compensation scheme on the FPGA platform. The results show that the compensation method can effectively reduce the sinusoidal error component in the signal, and the subdivision error is reduced from 0.95'' to 0.56'' in the time domain. Consequently, the zero-order, first-order, second-order and third-order components are considerably suppressed. The compensation scheme can realize the sinusoidal error compensation of the grating moiré signal and effectively improve the measurement accuracy of the grating encoder.

INDEX TERMS Photoelectrical encoder, moiré fringe, Sinusoidal error compensation, particle swarm optimization, FPGA implementation.

I. INTRODUCTION

Gratings are the standard sensors for the measurement of angular displacement and are widely used in diverse scientific and industrial applications such as precision engineering, aerospace, optics, angle-measuring standards, etc. [1]–[4]. The resolution of a grating device depends on the grating pitch. Due to the technical limitations of grating production and the requirements of measurement resolution, subdividing the photoelectric signal of the grating moiré becomes an important part of the grating measurement.

The method of subdividing the grating moiré signal is roughly classified into two categories: subdivision based on phase and subdivision based on amplitude [5]–[7]. In the actual application process, the digital subdivision method based on amplitude has better flexibility and is more widely used [8]. During the measurement process, due to the influence of factors such as installation and environment, the moiré signal usually includes errors such as direct current (DC) offset, equal amplitudes of constituent signals, orthogonality of two signals and the harmonic components of the moiré fringe signal [9], [10]. Among them, the DC offset of the signal introduces a single-cycle non-sinusoidal subdivision error; the equal amplitude error of the signal introduces a double-cycle approximately-sinusoidal subdivision error; the quadrature error of the signal introduces a subdivision error, whose value can go up to the phase difference of the two signals (between 0° and 180°); the sinusoidal deviation

The associate editor coordinating the review of this manuscript and approving it for publication was Yassine Maleh.

of the signal introduces the corresponding subdivision error according to the content of each harmonic [11]. These errors affect the effect of subdivision; therefore, it is necessary to improve signal quality through the compensation system during the implementation of subdivision.

Because the DC offset of the signal, the equal amplitude error, the quadrature error existing in the time domain of the signal and the sinusoidal error of the signal quantified in the frequency domain, the sinusoid error compensation is more difficult to achieve compared to the other three errors. Traditionally, the methods for reducing the sinusoidal error of the grating moiré signal are mainly divided into two categories: one is to change the structure of the photoelectric encoder, and the other is to use a software compensation method in the circuit.

The methods for changing the structure of photoelectric encoders are as follows: Reference [12] proposed a method of spatial filtering, which increases the filtering of higher harmonics by adding a filtering diaphragm; literature [13] proposed a phase difference filtering method to weaken the components of higher harmonics considering the different phase arrangement relationships between the upward combinations of the indicating gratings, thereby improving the quality of the moiré signal. However, these methods complicate the structure of the encoder, and demand higher requirements for the optical system; therefore, these methods are not suitable for this study.

The software compensation method mostly uses the fitting algorithm to solve the signal waveform equation; based on this, the deviation correction method is performed. Heydemann first proposed the automatic compensation technique of the moiré fringe photoelectric signal based on the least squares fitting method [14]. The least squares method is used to solve uncertain parameters in the signal model, its estimation is unbiased and uniformly converged only when under the condition of white noise with stationary zero mean. Therefore, future generations have done numerous researches and improvements based on this method.

As in [15], the Lissajous figure mapping method is proposed to indirectly reduce the influence of sinusoidal deviation on the subdivision error. However, when the signal contains higher harmonic components, the Lissajous figure observation method cannot accurately reflect the signal quality. In the literature [16], the method of series compensation for the subdivision error of the encoder using the ellipse fitting method is proposed for the Lissajous figure.

Besides, to overcome the problem of non-convergence of the least squares method, a sinusoidal correction method based on the empirical mode decomposition is proposed in [17]. Using the principle of empirical mode decomposition, the fundamental signal in the grating moiré signal is extracted for the purpose of eliminating harmonics. However, this method needs to obtain the signal fundamental frequency by using the absolute encoder coarse code information, hence the application is limited. In [18], a compensation method based on a tuneable digital filter is designed to suppress the harmonic components of the subdivided signal, and the frequency problem of the moiré signal is solved. However, the filtering effect of this method varies with the fundamental frequency and is more suitable for high-frequency signals. Literature [19] proposes a sinusoidal error compensation method based on particle swarm optimization (PSO). The PSO algorithm is used to solve two signal waveform parameters to further realize the signal sinusoidal error compensation. However, the waveform equation and the adaptive inertia weight change method are complex, which increases the complexity of the PSO algorithm and is more suitable for algorithm implementation on the DSP platform. Moreover, in terms of parameter solving algorithms, some scholars have applied Newton's iteration method, genetic algorithm, cuckoo search algorithm and other methods to the solution of signal waveform parameters [20]–[23]. However, these methods have the defects of complex calculation, low parameter applicability, and slow implementation speed.

After comprehensively comparing the above-mentioned compensation algorithms and based on the compensation principle of [19], this paper establishes a simpler waveform equation based on the spectral characteristics of the grating signal. At the same time, the inertia weight change mode in the literature is simplified, and the complexity of the PSO fitting algorithm is finally reduced. Finally, the PSO algorithm is used to solve the waveform equation parameters and the signal sinusoidal error compensation on the field-programmable gate array (FPGA) platform. It is verified by the experiments that the compensation scheme effectively improves the subdivision accuracy of the grating moiré fringe photoelectric signal. For gyroscope signals of the same type as the grating moiré signal, existing drift compensation methods include a method of combining an autoregressive (AR) model or an auto regressive moving average (ARMA) model with a Kalman filter, and the support vector machine (SVM) method. However, the former requires the time series to have stability, normality and independence, which greatly limits the range of use and prediction accuracy of the model. In the latter, the overall error of the signal is compensated, and in the process of sinusoidal error compensation, fixed harmonic components need to be specifically removed, hence this method cannot achieve this function.

The rest of the paper is organized as various sections. Section II introduces the principle of grating measurement and analysis various sources of error, besides, introduces the principle of moiré signal subdivision and the influence of sinusoidal error. Section III introduces the principle of sinusoidal error compensation and the application of the PSO algorithm in waveform equation solving. Section IV introduces the key issues of the compensation algorithm in the FPGA implementation process. Section V introduces the experimental results of the compensation algorithm applied to the fixed signal generator output signal and the actual grating encoder. Finally, conclusions are derived in Section VI.

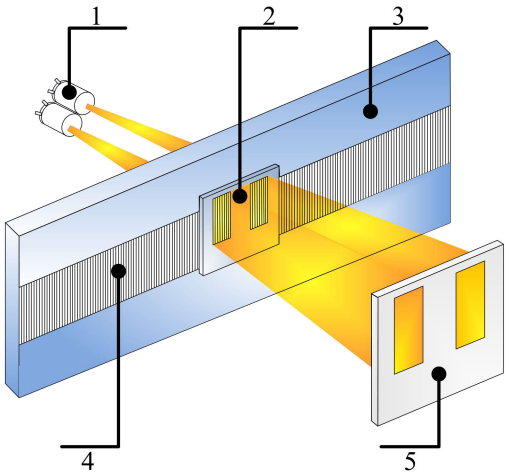

FIGURE 1. Grating measurement system structure.

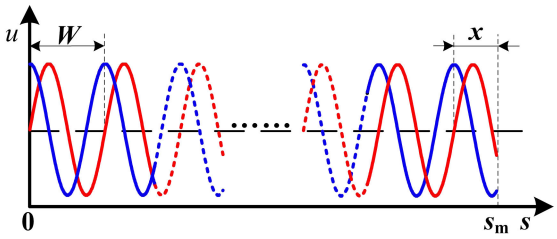

FIGURE 2. Output signal waveform.

II. INFLUENCE OF SINUSOIDAL ERROR ON GRATING MEASUREMENT

A. GRATING MEASUREMENT PRINCIPLE AND SOURCE OF SIGNAL ERROR

The grating measurement system is mainly composed of the main grating, indicating grating, light source, and photoelectric element [24]. During the measurement process, moiré fringes are generated by the relative movement of the main grating and the indicating grating, and the two sine and cosine electrical signals that differ by 90° are output by the photoelectric element. The measurement system structure is shown in Figure 1. In the figure, 1 is a light source, 2 is an indicating grating, 3 is the main grating, 4 is the grating reticle and 5 is a photoelectric receiving element.

The period of the grating moiré signal corresponds to the grating pitch. When the relative displacement between the main grating and the indicating grating is S_{m}, the waveform of the output moiré signal is shown in Figure 2.

The movement displacement of the grating sensor is:

$$S_m = nW + x \tag{1}$$

In the formula, n is the number of grating moiré signal moving cycles, W is the grating pitch and x is the displacement within the grating pitch. Among them, n is obtained by cycle counting and x is measured by signal subdivision.

From Figure 1, during the measurement process, the characteristics of the grating pair, light source, photoelectric element, installation and debugging, application environment and other factors affect the grating moiré signal, thereby affecting the moiré signal subdivision effect. The sources of errors are shown in Table 1.

TABLE 1. Sources of grating signal errors.

	DC offset	Equal amplitude error	Quadrature error	Sinusoid error
grating pair	√	√		√
Lighting system	√	√	√	√
Receiving system	√	√		√
application environment	√	√	√	√
installation and debugging		√	√	√

It can be seen from Table 1 that sinusoidal error is easily affected by more factors. In practical application scenarios, the grating moiré signal must include sinusoidal error. Therefore, in the field of precision measurement with high-resolution requirements, an appropriate compensation for the sinusoidal error of the signal is necessary.

B. PRINCIPLE OF ARCTANGENT SUBDIVISION OF GRATING MOIRÉ SIGNAL

Arctangent subdivision is one of the most commonly used digital subdivision methods. This method completes the subdivision task based on the correspondence between the amplitude and phase of the moiré signal. For two ideal grating signals, the expression is:

$$\begin{cases} u_1(\theta) = A\sin\theta \\ u_2(\theta) = A\cos\theta \end{cases} \tag{2}$$

Within a range of grating pitch, the fixed measuring position corresponds to the phase of the sine and cosine signals. When the subdivision value in a grating pitch is S, the measured position corresponds to the subdivision output value s, which is expressed as:

$$s = \mathrm{int}\left(\frac{\theta}{2\pi} \cdot S\right) \tag{3}$$

The digital subdivision task is employed to obtain the phase θ of the compensated grating signal. Because the amplitude-phase correspondence of sinusoidal signals is nonlinear, it is necessary to calculate the phase of the signals. To achieve this, we define the function $u(\theta)$ as:

$$u(\theta) = \begin{cases} \tan\theta = \dfrac{|A\sin\theta|}{|A\cos\theta|} & |A\sin\theta| \le |A\cos\theta| \\ \cot\theta = \dfrac{|A\cos\theta|}{|A\sin\theta|} & |A\sin\theta| > |A\cos\theta| \end{cases} \tag{4}$$

Let $u_1'(\theta) = |A\sin\theta|$, $u_2'(\theta) = |A\cos\theta|$. According to formula (4), Figure 3 shows the comparison among $u_1'(\theta)$, $u_2'(\theta)$ and $u(\theta)$.

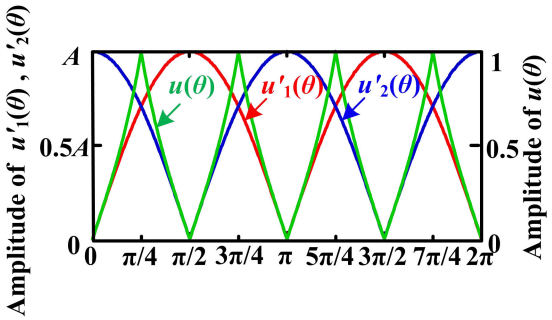

FIGURE 3. Comparison among original signals and constructed function.

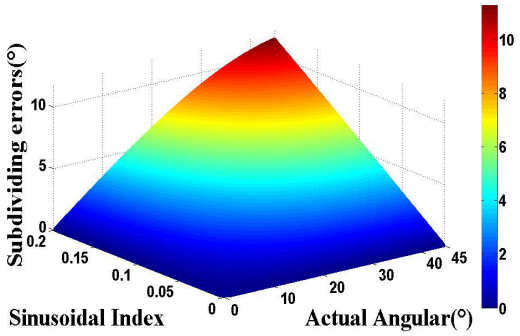

FIGURE 4. Subdivision error introduced by signal sinusoidal error.

TABLE 2. Calculation formulas of each phase interval.

Interval number	s	Interval number	s
1	$\frac{S\times acr\tan\frac{A\sin\theta}{A\cos\theta}}{2\pi}$	5	$\frac{S}{2}+\frac{S\times acr\tan\frac{A\sin\theta}{A\cos\theta}}{2\pi}$
2	$\frac{S}{4}-\frac{S\times acr\tan\frac{A\cos\theta}{A\sin\theta}}{2\pi}$	6	$\frac{3S}{4}-\frac{S\times acr\tan\frac{A\cos\theta}{A\sin\theta}}{2\pi}$
3	$\frac{S}{4}+\frac{S\times acr\tan\frac{A\cos\theta}{A\sin\theta}}{2\pi}$	7	$\frac{3S}{4}+\frac{S\times acr\tan\frac{A\cos\theta}{A\sin\theta}}{2\pi}$
4	$\frac{S}{2}-\frac{S\times acr\tan\frac{A\sin\theta}{A\cos\theta}}{2\pi}$	8	$S-\frac{S\times acr\tan\frac{A\sin\theta}{A\cos\theta}}{2\pi}$

Signal $u(\theta)$ can be divided into 8 intervals using the crossover and zero-crossing points of the two moiré signals and by performing an arctangent calculation. Finally, the corresponding subdivision output value is calculated according to the interval number. The relationship between the interval number and the subdivision output value is shown in Table 2.

C. INFLUENCE OF SIGNAL SINUSOIDAL DEVIATION ON SUBDIVISION ERROR

The ideal grating moiré signal is two sine and cosine signals without errors. However, due to the processing defects of the grating encoder, there are harmonics in the actual output grating moiré fringe photoelectric signal. Using the harmonics to form the grating stripe photoelectric signal output by the photoelectric encoder:

$$\begin{cases} u_{\sin}(\theta) = A_0 + A_1\sin(\theta) + \cdots + A_n\sin(i\theta) \\ u_{\cos}(\theta) = B_0 + B_1\cos(\theta) + \cdots + B_n\cos(i\theta) \end{cases} \tag{5}$$

In the formula, A_i, B_i $(i = 0, 1, 2\cdots n)$ respectively represent the amplitudes of the harmonics of the sine and cosine signals. η is defined as the sinusoidal index representing the harmonic content of the signal.

$$\eta = \frac{\sum_{i=0}^{n} A_i}{A_1} \tag{6}$$

Normally, the amplitude of each harmonic in the grating moiré signal is not more than 20% of the amplitude of the fundamental wave. According to the principle of arctangent subdivision, the one-cycle grating moiré signal is divided into 8 intervals, and the angle value of each interval is about 45°. The angular error is calculated within the actual corner value $\theta \in [0°, 45°]$ in the range of $\eta \in [0, 0.2]$. The obtained sine index and angle error curve are shown in Figure 4.

According to the results of the above figure, the larger the sine index η, the more apparent the trend of subdivision error changes with the theoretical angle. When the sine index η reaches the maximum value of 0.2, the maximum subdivision error in the range of the theoretical angle 0°-45° reaches 11.3030°. According to formula (2), when the number of subdivisions $S = 1,024$, the corresponding subdivision number is calculated to be 32.

That is, the angular error introduced by the signal sinusoidal error will result in an error of 32 subdivisions when the subdivision number is 1,024. The sinusoidal error in the signal affects the result of the final subdivision, and the larger the sine index, the more obvious the impact on the subdivision result.

III. COMPENSATION PRINCIPLE OF PARTICLE SWARM OPTIMIZATION FOR SINUSOIDAL ERRORS

A. ERROR COMPENSATION PRINCIPLE

On the premise of obtaining the two-channel grating moiré signal waveform equation, by calculating the harmonic content in the signal and then removing the harmonic content of the waveform signal in the time domain, the sinusoidal error compensation of the grating moiré signal is obtained as shown in Figure 5.

It can be seen from Figure 5 that after sampling the grating moiré signal, two sine and cosine signals with sinusoidal errors are obtained. When the grating signal waveform equation is obtained, the harmonic content corresponding to each sampling point can be calculated and the signal can be compensated. The compensated grating moiré signal is subdivided by the signal to finally obtain the correct number of subdivisions.

Among them, the harmonic content $u_{\sin\Delta}(\theta)$ and $u_{\cos\Delta}(\theta)$ are expressed as:

$$\begin{cases} u_{\sin\Delta}(\theta) = A_0 + A_2\sin(2\theta) + \cdots + A_i\sin(i\theta) \\ u_{\cos\Delta}(\theta) = B_0 + B_2\cos(2\theta) + \cdots + B_i\cos(i\theta) \end{cases} \tag{7}$$

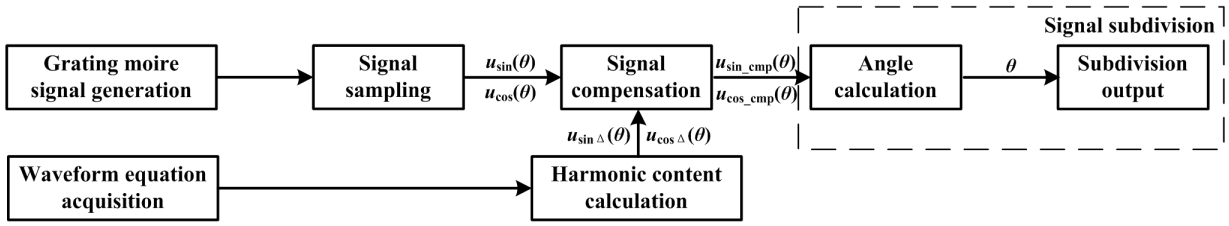

FIGURE 5. Signal compensation method flowchart.

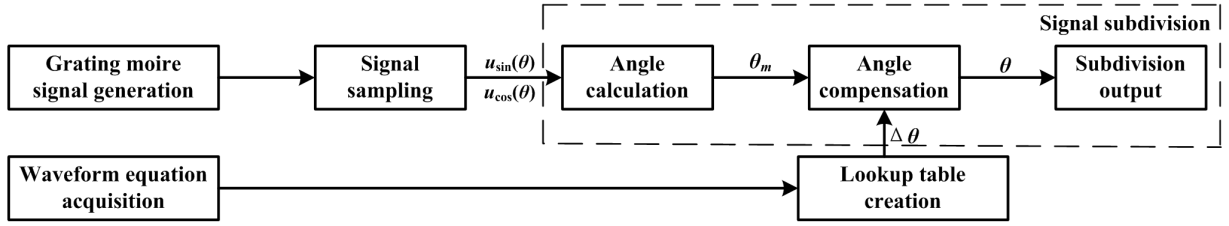

FIGURE 6. Angle compensation method flowchart.

The signal error compensation formula is:

$$\begin{cases} u_{\sin\_cmp}(\theta) = u_{\sin}(\theta) - u_{\sin\Delta}(\theta) \\ u_{\cos\_cmp}(\theta) = u_{\cos}(\theta) - u_{\cos\Delta}(\theta) \end{cases} \tag{8}$$

When directly compensating the signal, it is necessary to calculate and compensate the harmonic content of the angular position of each sampled data. The complexity of sine and cosine calculations and the large amount of data to be compensated under high-frequency sampling directly affects the resource occupation of the code and the real-time nature of signal compensation.

To reduce resource occupation and delay caused by the signal sine and cosine calculation, this study quantifies the angle error value introduced by signal harmonics and uses the table lookup compensation method to directly compensate the sinusoidal error of the subdivided calculation output angle. The angle compensation method flowchart is shown in Figure 6.

It can be seen from Figure 6 that in the angle compensation method, the two sine and cosine signals with sinusoidal errors obtained after sampling are directly subdivided into signals, that is, the angle values containing error components are obtained after the signals are subjected to angle calculation. Thereafter, an angle error compensation lookup table is established according to the obtained waveform equation, and the angle is compensated. The angle value after compensation is converted into the number of subdivisions for the output, and finally, the correct number of subdivisions is obtained. The angle error compensation formula is:

$$\theta = \theta_m - \Delta\theta \tag{9}$$

Among them, θ_m represents the angle value calculated from the uncompensated signal, and $\Delta\theta$ represents the angle error value introduced by the harmonics. Both can be calculated according to the arctangent subdivision principle.

The waveform equation of two signals is shown in formula (5). According to the principle of arctangent subdivision, the constructing tangent function is expressed as:

$$u'(\theta) = \begin{cases} \tan\theta_m = \dfrac{|u_{\sin}(\theta)|}{|u_{\cos}(\theta)|}, & |u_{\sin}(\theta)| \le |u_{\cos}(\theta)| \\ \cot\theta_m = \dfrac{|u_{\cos}(\theta)|}{|u_{\sin}(\theta)|}, & |u_{\sin}(\theta)| > |u_{\cos}(\theta)| \end{cases} \tag{10}$$

A schematic diagram showing the tangent function curves according to equations (4) and (10) is shown in Figure 7(a).

As seen from Figure 7(b), for any point $u'(\theta)$ (such as point b) in the function, the angle value calculated according to the tangent value (point b corresponds to the y-axis representation) is θ_m, and the point corresponds to the theoretical angle value θ. From this, the error value $\Delta\theta$ between θ_m and θ can be obtained:

$$\Delta\theta = \theta_m - \theta \tag{11}$$

In turn, the sinusoidal error can be compensated.

From this analysis, it is found that the sinusoidal error compensation of the grating moiré signal can be realized only by establishing a complete signal waveform equation and solving the position parameters therein.

B. DETERMINATION OF SIGNAL WAVEFORM EQUATION

According to the error compensation principle described in section A, to establish a lookup table between the measured angle value and the corresponding angle error value, it is necessary to obtain the waveform equation of the two signals to be compensated. This section establishes the signal waveform equation by analysing the harmonic components in the signal. On the actual grating measurement system platform,

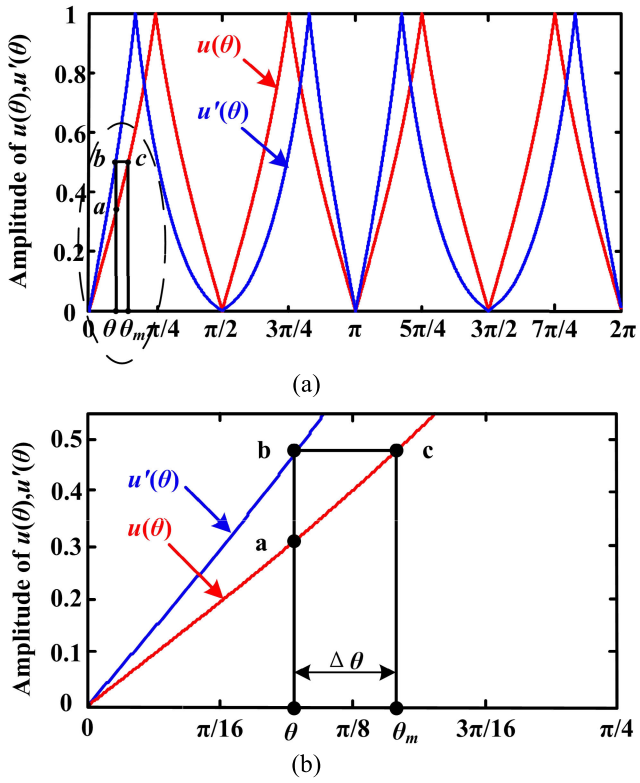

FIGURE 7. Schematic diagram of angular error caused by harmonics: (a) Schematic diagram of tangent curve containing harmonic components; (b) Schematic diagram of partial enlargement.

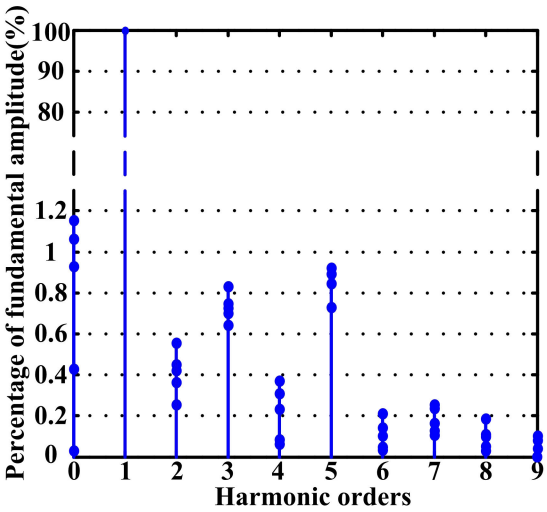

FIGURE 8. Grating moiré signal spectrum.

the FPGA circuit board is used to uniformly collect 5 sets of discrete signals to be compensated, and the Fourier spectrum analysis is used to obtain the magnitude of each harmonic amplitude as shown in Figure 8.

According to the spectrum analysis result of Figure 8, in the grating moiré signal, the zero-order harmonic, second harmonic, third harmonic and fifth harmonic amplitude account for the maximum value of the fundamental wave amplitude are greater than 0.4%; moreover, the maximum ratio of the residual harmonic amplitude to the fundamental amplitude is less than 0.4%. Therefore, the main harmonic order in the signal is considered to be zero-order, second-order, third-order and fifth-order, thereby determining the waveform equation of equation (12).

$$\begin{cases} u'_{\sin}(\theta) = A_0 + A_1\sin(\theta) + A_2\sin(2\theta) \\ \qquad\quad + A_3\sin(3\theta) + A_5\sin(5\theta) \\ u'_{\cos}(\theta) = B_0 + B_1\cos(\theta) + B_2\cos(2\theta) \\ \qquad\quad + B_3\cos(3\theta) + B_5\cos(5\theta) \end{cases} \tag{12}$$

According to the analysis in Section A, to eliminate the DC and harmonic components existing in the signal, it is necessary to solve five unknown parameters in the two signal waveform equations separately.

C. PRINCIPLE OF WAVEFORM PARAMETER SOLVING BASED ON PSO ALGORITHM

According to the two-way signal waveform equation established in Section B, to determine five unknown parameters, the PSO algorithm is used to fit the two signals separately. Taking the sin signal as an example, the nonlinear model of equation (13) is recorded as:

$$u'_{\sin}(\theta) = f(A_0, A_1, A_2, A_3, A_5) \tag{13}$$

Among them, A_0, A_1, A_2, A_3 and A_5 represent 5 unknown parameters in the waveform equation.

Here, 64 amplitude data are uniformly acquired in each grating period as U_1, U_2, $\cdots$, U_{64}. The cost function with the smallest squared error of the signal as the estimated parameter:

$$e = \min\left\{\sum_{i=1}^{64}(U_i - f(A_0, A_1, A_2, A_3, A_5))^2\right\} \tag{14}$$

Among them, fitness is defined as:

$$fitness = \sum_{i=1}^{64}(U_i - f(A_0, A_1, A_2, A_3, A_4))^2 \tag{15}$$

When the PSO algorithm is applied to the waveform parameter solution, the spatial position of each particle consists of five generation parameters. During the iterative process, the particles are iteratively updated according to the individual optimal position (p_{best}) and the global optimal position (g_{best}). The iteration formula is:

$$\begin{aligned} v_{im}(k+1) = {} & wv_{id}(k) + c_1r_1(p_{id}(k) - x_{id}(k)) \\ & + c_2r_2(g_d(k) - x_{id}(k)) \end{aligned} \tag{16}$$

$$x_{id}(k+1) = x_{id}(k) + v_{id}(k+1) \tag{17}$$

where k is the iteration number; d is the dimension, ie the number of independent variables; r_1 and r_2 are usually two independent and evenly distributed random numbers, and r_1, r_2 $\in$U(0,1); $x_{id}(k)$ is the d-th dimension component of

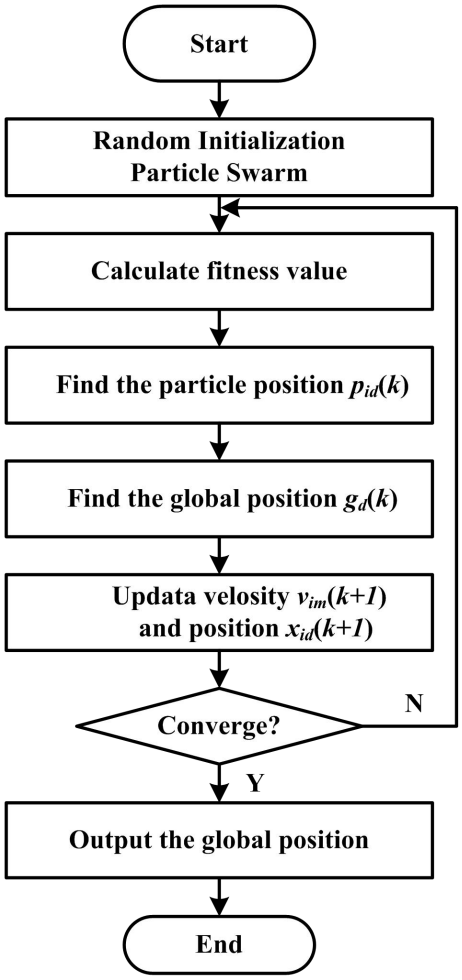

FIGURE 9. Particle swarm algorithm for waveform parameter solution.

the position vector at the k-th iteration of particle i; $p_{id}(k)$ represents the d-th dimension component of the best position vector of particle i in the first k iterations; $g_d(k)$ represents the d-th dimension component of the best position vector g_{best} of the entire group in the first k iterations; $v_{id}(k)$ is the d-th dimension component of the current velocity vector at the k-th iteration of the particle i; w is the inertia weight; and c_1 and c_2 are acceleration constants representing the weight of the statistical acceleration term that pushes each particle to the p_{best} and g_{best} positions, typically between 0 and 2.

The specific implementation flow chart of the PSO algorithm of parameter identification is shown in Figure 9.

According to the iterative formula of the PSO algorithm, the particles in the space gradually approach the position where the fitness value is the smallest. The algorithm judges the result of the PSO fitting based on the change of the fitness value. Finally, the particle position with the lowest fitness is the result of solving the waveform equation parameters.

IV. FPGA CIRCUIT IMPLEMENTATION OF PARTICLE SWARM OPTIMIZATION ALGORITHM

In the implementation of sinusoidal error compensation, because the PSO compensation algorithm requires higher resources and computing speed, FPGA is used as the hardware circuit bearing platform in the research, and the system performance requirements are met through the advantages of pipeline architecture and parallel computing. Besides, in order to more intuitively observe the effect of sinusoidal error compensation during the subdivision of the moiré signal of the grating, this article takes the 1024 subdivision of the moiré signal as an example and comparatively analyses the subdivision results before and after outputting the sinusoidal error compensation. The error situation is subdivided to reflect the effectiveness of the compensation algorithm.

In order to implement the angular error compensation method which shown in Figure 6 in FPGA, the key is to acquire the signal waveform equations (Waveform equation acquisition) and establish the lookup table creation and compensation (Angle compensation).

The design of the sinusoidal error compensation and subdivision circuit structure of the grating moiré signal is shown in Figure 10. Among them, the signal waveform equation acquisition part includes a uniform sampling of the preprocessed signal (Sample) and the application of the PSO algorithm to achieve the waveform parameter solution (PSO_sin/PSO_cos). The error compensation section includes the lookup table creation and the Sinu_comp section. Finally, according to the angle value before and after compensation, it is converted into 1024 subdivisions for subdivision output (Sub_1024).

During the implementation of the compensation algorithm, the accuracy of the waveform parameter solution (PSO_sin/PSO_cos) determines the effectiveness of the establishment of the error lookup table. Therefore, when implementing this module in the FPGA, the key is to solve the applicability of the parameter finding algorithm under actual application conditions. In the process of applying the PSO algorithm to solve the signal waveform parameters in the FPGA, due to the complexity of the PSO algorithm, various parameter settings directly affect the fitting accuracy of the algorithm and the resource occupation in the FPGA. In order to ensure the fitting accuracy of the algorithm on the premise of simplifying the algorithm and reducing the amount of resource consumption, this paper selects two important parameters that affect the fit of the PSO algorithm according to the algorithm fitting accuracy and resource occupation. Moreover, the lookup table creation and the compensation method (Sinu_comp) determine the compensation efficiency and compensation effect. Therefore, the key to this part in the implementation of the circuit is establishing a suitable lookup table and designing a fast and accurate lookup compensation method. This article establishes an error compensation lookup table based on the signal frequency and the FPGA code operating frequency. Finally, in order to achieve fast and accurate search, a method of combining shifting search and linear interpolation to perform error compensation is designed.

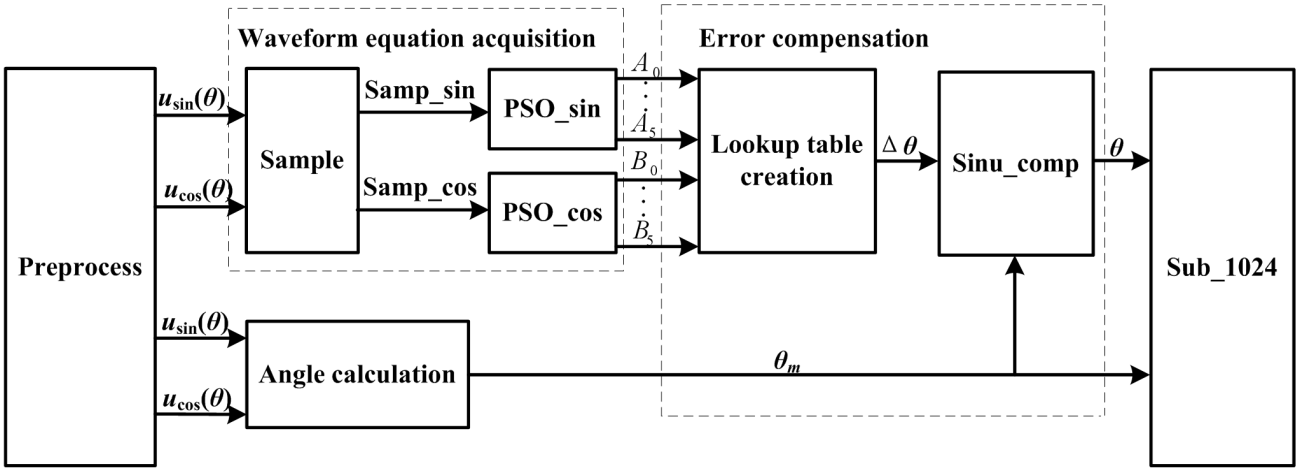

FIGURE 10. Circuit structure diagram of sinusoidal error compensation algorithm.

A. SELECTION OF INERTIAWEIGHT w

Inertia weight w plays a role in balancing the local optimal ability and the global optimal ability. The larger the w, the stronger the global search ability of the algorithm; conversely, a smaller w makes the search of the particle group more focused on the development of local regions [19], [20]. A commonly used formula for linear inertia weight variation is shown in equation (18).

$$w = w_{\max} - \frac{w_{\max} - w_{\min}}{iter_{\max}} \times k \tag{18}$$

where w_{max} is the inertia weight maximum, w_{min} is the inertia weight minimum, $iter_{max}$ is the maximum number of iterations, and k is the current number of iterations.

A nonlinear inertia weight change method is given in [18] as shown in equation (19).

$$w = \begin{cases} w_{\min}, & l < l_{\min} \\ w_{\max} - \dfrac{(l - l_{\min})(w_{\max} - w_{\min})k}{(l_{\max} - l_{\min})iter_{\max}}, & l_{\min} < l < l_{\max} \\ w_{\max}, & l > l_{\max} \end{cases} \tag{19}$$

where l_{max} and l_{min} are two preset parameters, which are represent the distance between the particle position and the global optimum in the current iteration.

To perform 1,000 PSO fitting for the two cases and record the fitness values of 1,000 fitting results, as shown in Figure 11, the following values are set: $w_{max} = 1$, $w_{min} = 0.4$, $l_{max} = 100$, $l_{min} = 10$ and $iter_{max} = 300$. It can be seen from the figure that when the linear inertia weight change mode is applied to the output signal of the encoder, the fitness value of the PSO fitting result is relatively stable, and the maximum is 7.103×10^4 in the 1,000 PSO fitting process. The fitness value of the PSO fitting results obtained by the nonlinear inertia weight change method proposed in the literature fluctuated greatly, with the maximum being 7.622×10^4. From the perspective of fitting accuracy, the linear inertia weight change mode has a higher accuracy and stability than the nonlinear inertia weight change mode.

TABLE 3. FPGA resource occupancy in the case of different inertia weight changes.

Number of particles	Spatial dimension	w change mode	LE
2	2	Linear inertia weight	2071
2	2	Nonlinear inertia weight	2345

Since the nonlinear inertia weight change method is more complicated, the amount of calculation of the algorithm increases when implemented on the FPGA platform. Here, taking the sine signal as an example, the resource occupancy of the PSO algorithm implemented on the FPGA platform using the two inertia weight change modes is shown in Table 3. According to Table 3, the FPGA resource occupancy is analysed. For the PSO fitting algorithm with 2 spatial dimensions and 2 particles, the resource occupied by the PSO algorithm using the linear inertia weight change method is smaller than the resource occupied by the PSO algorithm realized by the nonlinear interest weight change mode.

Compared with the analysis of the comprehensive fitting accuracy and the occupancy of the FPGA resources, the nonlinear inertia weight change method proposed by the literature is more complex and the fitting effect is worse in the application scenario of this paper. Therefore, the variation of inertia weight selected in this paper is the linear inertia weight change mode.

B. SELECTION OF THE NUMBER OF PARTICLES N

In general, a larger population size is conducive to the global exploration of the search space by particle swarms, while a smaller population size is more conducive to the development of local swarms. The PSO fitting calculation of one grating moiré signal is performed on the Matlab platform. The appropriate number of particles N was selected according to the stability of the algorithm. The initial position and initial velocity

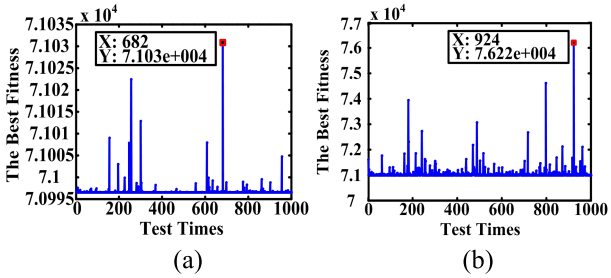

FIGURE 11. Solution of the fitness of different inertia weight changes: (a) Solution of the linear inertia weight change mode. (b) Solution of the nonlinear inertia weight change mode.

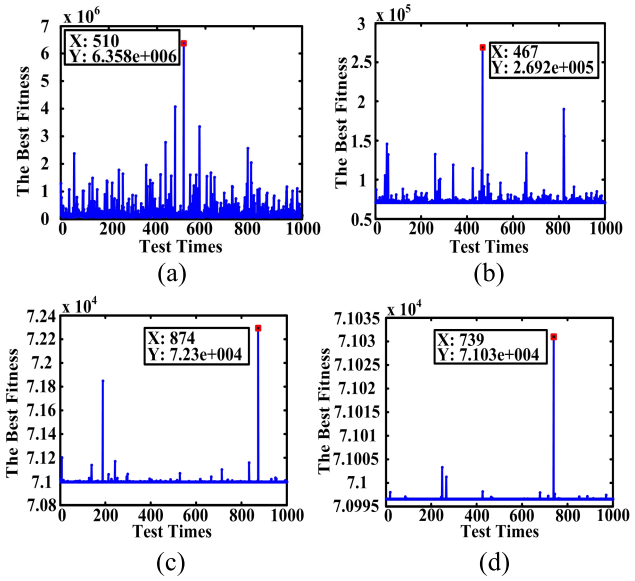

FIGURE 12. Solving the fitness of different particle numbers: (a) Fitness solution when $N = 5$. (b) Fitness solution when $N = 10$. (c) Fitness solution when $N = 20$. (d) Fitness solution when $N = 30$.

of the particles were randomly selected within a range, and 1,000 PSO fittings were performed for $N = 5, 10, 15$, and 20. The extent to which the initial position and velocity of the particles affect the PSO fit results for different particle counts were verified. The experimental results are shown in Figure 12.

It can be seen from Figure 12 that when $N = 5$, the PSO fitting results fluctuate greatly with the initial position and velocity of the particles and the optimal fitness value of the fitting result reaches 6.358×10^6. When $N = 10$, the optimal fitness value of the PSO fitting result reaches 2.692×10^4, and the fitting result remains dependent on the initial position of the particle. When $N = 20$, the optimal fitness value of the fit is 7.23×10^4, and the range of fitness value fluctuation is small. When $N = 30$, the optimal fitness value of the fit is 7.103×10^4, and the range of fitness value fluctuation is the smallest. That is, from the fitting accuracy analysis, the fitting precisions of $N = 20$ and $N = 30$ are similar.

The resource occupancy of different numbers of particles on the FPGA platform is shown in Table 4.

TABLE 4. FPGA resource occupancy in the case of different particle counts.

Number of particles	Spatial dimension	w change mode	LE
5	5	Linear inertia weight	5019
10	5	Linear inertia weight	7321
20	5	Linear inertia weight	12651
30	5	Linear inertia weight	18093

TABLE 5. Sinusoidal error compensation lookup table.

addr	0	1	2	⋯	*M-1*	*M*
θ_s	0	θ'	$2\theta'$	⋯	$(M\text{-}1)\theta'$	$M\theta'$
$\Delta\theta$	Δ_0	Δ_1	Δ_2	⋯	$\Delta_{M\text{-}1}$	ΔM

According to Table 4, the resource occupancy of the FPGA increases with the number of particles. When the number of particles is $N = 20$ and $N = 30$, resource occupancy differs by 5,442LE.

According to the analysis of the PSO fitting accuracy and resource occupancy, the fitting accuracy of $N = 20$ does not vary greatly from that of $N = 30$, but the resource occupancy of $N = 30$ is more than that of $N = 20$. Therefore, the number of particles selected in this paper is $N = 20$.

C. ERROR COMPENSATION MODULE IMPLEMENTATION

After obtaining the waveform parameter fitting result, a lookup table for calculating the angle value θ_s and the angle error $\Delta\theta$ can be established according to the complete waveform equation. In turn, the table lookup compensation for sinusoidal errors is implemented on the FPGA platform. In the error compensation process, it is essential to solve the problem of establishing the lookup table to achieve a more accurate compensation effect. In the establishment of the angle error lookup table, the angular error must first be accurately found by looking up the table address. The lookup table established in this paper is shown in Table 5.

Where *addr* is the lookup table address, θ' is the lookup table angle interval, and M is the lookup table maximum address. The lookup table spacing θ' is related to the amplification factor q of the calculated angle value θ_m before the sinusoidal error compensation, the signal frequency f, and the code running clock frequency F. Its calculation formula is as follows:

$$\theta' \leq \frac{360 \times q \times f}{F} \tag{20}$$

To facilitate the corresponding lookup of the angle θ_m to the lookup table address on the FPGA, $\theta' = 2^{\mathrm{n}}$ is required, where n is a positive integer.

The angle error address of θ_m is searched as follows:

$$addr_1 = \left\lfloor \frac{\theta_m}{\theta'} \right\rfloor \tag{21}$$

$$addr_2 = addr_1 + 1 \tag{22}$$

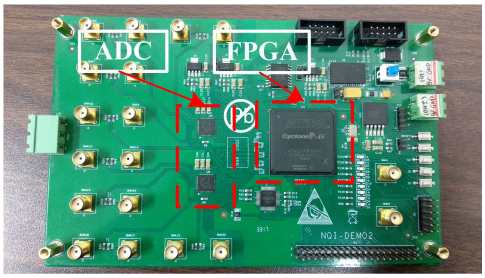

FIGURE 13. FPGA board.

The angular error can be calculated using linear interpolation:

$$\Delta_z = \frac{\theta_m - addr_1\theta'}{\theta'}(\Delta_{addr2} - \Delta_{addr1}) + \Delta_{addr1} \quad (23)$$

The angle compensation formula is:

$$\theta'_m = \theta_m - \Delta_z \quad (24)$$

According to the above error finding table establishment and compensation mode, the sinusoidal error compensation of the grating moiré signal can be realized on the FPGA circuit.

V. EXPERIMENT AND DATA ANALYSIS

In order to prove the effectiveness of the sinusoidal error compensation system, the actual signal was loaded on the self-made FPGA circuit to verify the subdivision function. The circuit board is shown in Figure 13. Among them, a 16-bit ADC chip with a sampling rate of 40 MSa/s was used to obtain the grating moiré fringe photoelectric signals. While ensuring that the number of the FPGA resources can meet the code requirements, a low-cost Altera Cyclone E series chip (EP4CE10F17C8) was used to implement the compensation algorithm. In the Quartus development environment, the Verilog language was used to design the compensation algorithm circuit and was downloaded into the FPGA chip to complete the compensation task.

A. VALIDATION OF THE VALIDITY OF THE SINUSOIDAL ERROR COMPENSATION SCHEME

In this section, we compare the subdivision results of the deterministic signals generated by the signal generator before and after compensation. The signal generator set the signal frequency to 10 KHz, and the set signal contained 0th to 13th order harmonic components. The AD sampling frequency in the board was 20 MHz. We used an FPGA board to cache the results of subdivision into the RAM (random access memory) of the FPGA chip. The experimental results are shown in Figure 14, where the unit of the curve is the subdivision value (which corresponds to 1024 subdivisions). In Figure 14(a), the results of subdivision within a sinusoidal signal period are shown, where the curves before and after compensation overlap and show a linearly increasing trend. For a constant signal frequency, the output subdivision results should also exhibit a linear increase. To illustrate the minor

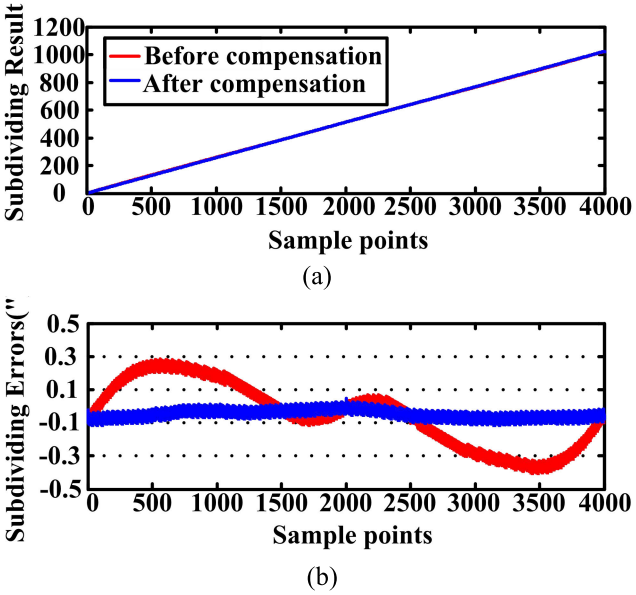

FIGURE 14. Subdivision error of signal generator signal before and after sinusoidal error compensation: (a) Subdivision results before and after sinusoidal error compensation. (b) Subdivision error results before and after sinusoidal error compensation.

differences between the two curves, we define the linearity error as the deviation between the results and an ideal uniform line, which is used as a reference.

The obtained compensation effect is shown in Figure 14(b), in which the subdivision error result is converted into a whole circular subdivision error according to the 16384-line raster code disc. The compensated subdivision error peak-to-peak value was 0.14'', and the subdivision error peak-to-peak value before compensation was 0.7''. The uniformity of the number of subdivisions after compensation is significantly better than that before compensation. It was found that for two sine and cosine signals with only harmonic errors, the sinusoidal error compensation method can be used to effectively compensate. The experimental results show that the subdivision error is significantly reduced, which proves the effectiveness of the sinusoidal error compensation scheme based on the PSO algorithm.

B. CALIBRATION OF SUBDIVISION ACCURACY

This part verifies the sinusoidal error compensation effect of the actual grating moiré signal. The encoder is a Micro E Encoder Sensor (M20) and a Standard Rotary Scales (R10851). The grating disk and the reading head were mounted on the air-floating turntable bearing structure, and the physical diagram of the device is shown in Figure 15. The angle measurement result of the autocollimator was used as the actual angle value. The error compensation and subdivision processing of the actual grating signal were made using a self-made circuit.

Table 6 shows the specifications of the main instruments used in this experiment. During the experiment, one of the pitches was selected for subdivision accuracy calibration. The

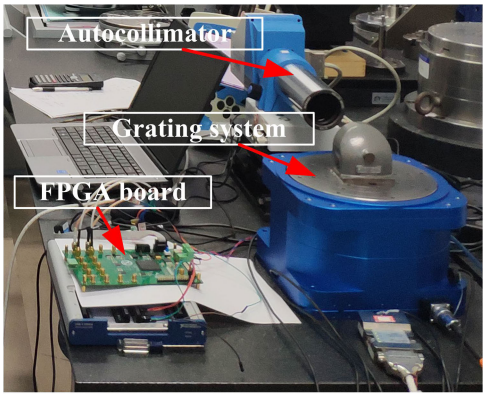

FIGURE 15. Schematic of the experimental set up.

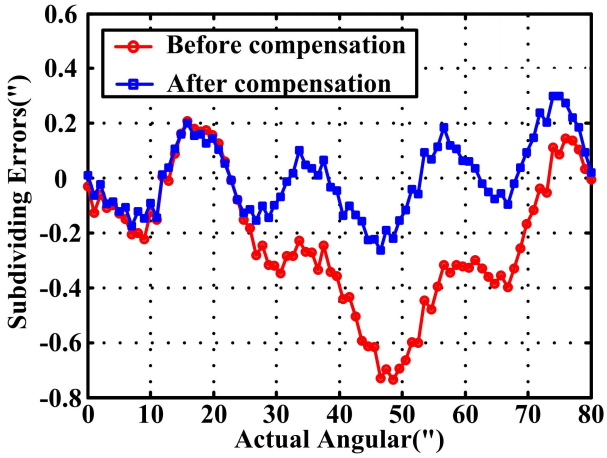

FIGURE 16. Calibration errors of angle measurement.

step motion of the turntable was set to 1'' and the measurement angle range to 80''. A total of 80 sample points were recorded. Using the NI card, both the angle measurement results of the autocollimator and the angle measurement results before and after the sinusoidal error compensation were obtained. The calibration error of the angular displacement is shown in Figure 16.

The maximum subdivision error obtained by the grating moiré signal before the sinusoidal error compensation is 0.21'', the minimum subdivision error is −0.74'', and the peak-to-peak value is 0.95''. The maximum subdivision error of the measured angle value after compensation is 0.30'', the minimum subdivision error is −0.26'', and the peak-to-peak value is 0.56''. The subdivision error is reduced by 41%.

Fourier spectrum analysis was performed on the results of the subdivision error before and after the compensation shown in Figure 16, and the results are shown in Figure 17. It can be seen from Figure 17 that before the sinusoidal error compensation, the zero-order, first-order, second-order, third-order, and fourth-order components in the signal subdivision error spectrum are obvious. After compensation, the zero-order, first-order, second-order and third-order components are effectively suppressed, and the subdivision error of the signal is significantly reduced as a whole.

TABLE 6. Specifications of the main instruments.

Instrument	Model (manufacturer)	Specification
Autocollimator	ELCOMAT 3000	Measuring range: From -1000″to+1000″ U_i=0.25″
Rotary glass scales	R10851 (Micro E system)	16384 CPR grating pitch: 20 μm
Reading head	Mercury's sensor (Micro E system)	Rotary: up to ± 2.1"(arc sec)

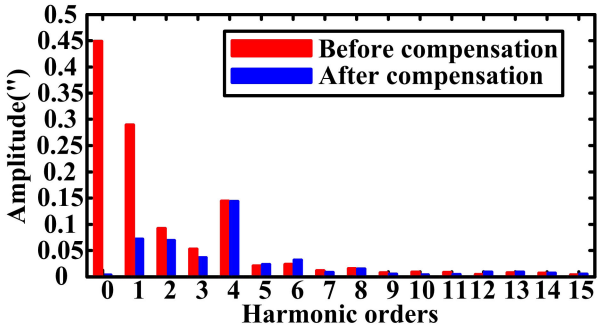

FIGURE 17. Spectrum results of the subdivision error before and after sinusoidal error compensation.

From the analysis of the results of the subdivision errors in the time and frequency domains, it can be known that the sinusoidal error compensation scheme of the grating moiré signal proposed in this paper is effective and feasible, the error compensation effect is obvious, and the subdivision accuracy is further improved.

VI. CONCLUSION

In this paper, the sinusoidal error compensation method for the grating moiré fringe photoelectric signal is studied. The sinusoidal error compensation system is constructed based on the FPGA circuit. First, the angle compensation scheme for sinusoidal error compensation was determined. Secondly, the waveform equations of DC, second harmonic, third harmonic and fifth harmonic were established, and the parameters of the waveform equation were solved on the FPGA platform by PSO algorithm. Thereafter, two key parameters such as inertia weight w and particle number N were selected, which reduced the complexity of the algorithm and saved the FPGA resources to a maximum while ensuring fitting accuracy. Subsequently, according to the waveform equation parameters combined with the subdivision model, the subdivision error compensation lookup table was designed to realize the signal sinusoidal error compensation. In the experimental process, the sinusoidal error compensation of the

harmonic-only sine and cosine signals generated by the signal generator was proved first, and then the effectiveness of the compensation model was proved. Thereafter, the compensation scheme was applied to the actual grating moiré signal. The experimental results show that the subdivision error is reduced from 0.95'' to 0.56'', and the angle measurement accuracy has considerably improved. The sinusoidal error compensation scheme designed in this study, which was implemented on the FPGA platform is feasible and flexible when applied to the sine and cosine signals output by the photoelectric encoder.

REFERENCES

[1] Y. Huang, Z. Xue, M. Huang, and D. Qiao, ''The NIM continuous full circle angle standard,'' *Meas. Sci. Technol.*, vol. 29, no. 7, Jul. 2018, Art. no. 074013.

[2] Y. Huang, Z. Xue, D. Qiao, Y. Wang, ''Study on the metrological performance of self-calibration angle encoder,'' *Proc. SPIE*, vol. 9684, Sep. 2016, Art. no. 96840O.

[3] W. Kokuyama, T. Watanabe, H. Nozato, and A. Ota, ''Measurement of angle error of gyroscopes using a rotary table enhanced by self-calibratable rotary encoder,'' in *Proc. IEEE Int. Symp. Inertial Sensors Syst. (ISISS)*, Mar. 2015.

[4] W. Ren, J. Cui, and J. Tan, ''A novel enhanced roll-angle measurement system based on a transmission grating autocollimator,'' *IEEE Access*, vol. 7, pp. 120929–120936, 2019.

[5] Z. Chen, X. Liu, D. Peng, Y. Zheng, X. Chen, and F. Zheng, ''Dynamic model of NC rotary table in angle measurements with time series,'' *Trans. Inst. Meas. Control*, vol. 35, no. 2, pp. 181–187, Apr. 2013.

[6] G. Ye, S. Fan, H. Liu, X. Li, H. Yu, Y. Shi, L. Yin, and B. Lu, ''Design of a precise and robust linearized converter for optical encoders using a ratiometric technique,'' *Meas. Sci. Technol.*, vol. 25, no. 12, Dec. 2014, Art. no. 125003.

[7] M. Benammar, ''A novel amplitude-to-phase converter for sine/cosine position transducers,'' *Int. J. Electron.*, vol. 94, no. 4, pp. 353–365, Apr. 2007.

[8] M. M. Elgaud, M. S. D. Zan, A. A. Ghaith, A. A. A. Bakar, N. Arsad, N. F. Naim, and M. H. H. Mokhtar, ''Improving the signal-to-noise ratio of time domain fiber Bragg grating sensor based on hybrid simplex and Golay coding technique,'' *IEEE Access*, vol. 7, pp. 167089–167098, 2019.

[9] G. Y. Ye, Y. S. Shi, L. Yin, H. Z. Liu, X. Li, H. Y. Yu, and B. H. Lu, ''Analysis of quadrature phase-shift error caused by angular misalignment in moiré linear encoders,'' *Adv. Mater. Res.*, vols. 712–715, pp. 1863–1867, Jun. 2013.

[10] W. Zhu, S. Ye, Y. Huang, and Z. Xue, ''Design of a precise subdivision system for gratings using a modified CORDIC algorithm,'' *IET Circuits, Devices Syst.*, vol. 13, no. 8, pp. 1284–1291, Nov. 2019.

[11] X. Wang, ''Errors and precision analysis of subdivision signals for photoelectric angle encoders,'' *Opt. Precis. Eng.*, vol. 20, no. 2, pp. 379–386, Feb. 2012.

[12] C. Wang, G. Zhang, and S. Guo, ''Autocorrection of interpolation errors in optical encoders,'' *Proc. SPIE*, vol. 2718, May 1996, Art. no. 240896.

[13] H. Wu, Q. Zeng, D. Qiao, and B. Guo, ''Filtering method for improving the quality of grating moiré fringe signal,'' *Opt. Precis. Eng.*, vol. 19, no. 8, pp. 1944–1949, Aug. 2011.

[14] P. L. M. Heydemann, ''Determination and correction of quadrature fringe measurement errors in interferometers,'' *Appl. Opt.*, vol. 20, no. 19, p. 3382, Oct. 1981.

[15] K. Tan, H. X. Zhou, and T. Heng Lee, ''New interpolation method for quadrature encoder signals,'' *IEEE Trans. Instrum. Meas.*, vol. 51, no. 5, pp. 1073–1079, Oct. 2002.

[16] X. Wang, J. Guo, and T. Xie, ''Elliptic fitting and subdivision correction algorithm for precision diffraction grating signal,'' *Tool Technol.*, no. 12, pp. 47–49, 2003.

[17] Y. Liu, H. Lu, and Y. Wang, ''Compensation method of moiré fringe sinusoidal deviation in satellite optical communication coarse pointing system,'' *J. Instrum.*, vol. 33, no. 8, pp. 1735–1740, 2012.

[18] Y. Wang, Y. Liu, X. Yan, X. Chen, and H. Lv, ''Compensation of moiré fringe sinusoidal deviation in photoelectrical encoder based on tunable filter,'' in *Proc. Symp. Photon. Optoelectron. (SOPO)*, May 2011.

[19] X. Gao, Q. Wan, X. Lu, and Y. Sun, ''Automatic compensation of sine deviation for grating fringe photoelectric signal,'' *J. Opt.*, vol. 33, no. 7, pp. 194–199, Jul. 2013.

[20] Y. Feng and Q. Wan, ''Interpolation error calibration method of small photoelectric encoders,'' *Chin. J. Sci. Instrum.*, vol. 34, no. 6, pp. 175–180, Jun. 2013.

[21] A. Avdeev and O. Osipov, ''PMSM identification using genetic algorithm,'' in *Proc. 26th Int. Workshop Electr. Drives: Improvement Efficiency Electr. Drives (IWED)*, Jan. 2019.

[22] F. Zheng, L. Yan, Q. Tang, Y. Zheng, and S. Jian, ''Research on parameter identification and compensation method of time-grating error based on genetic algorithm,'' *Chin. J. Sens. Actuators*, vol. 32, no. 10, pp. 1–8, Oct. 2019.

[23] H. H. Issa and S. M. Eisa Ahmed, ''FPGA implementation of floating point based cuckoo search algorithm,'' *IEEE Access*, vol. 7, pp. 134434–134447, 2019.

[24] X. Gao, S. Li, Q. Ma, and W. Chen, ''Development of grating-based precise displacement measurement technology,'' *Chin. Opt.*, vol. 12, no. 4, pp. 741–752, Aug. 2019.

[25] Y. H. Shi and R. C. Eberhart (1998), ''Parameter selection in particle swarm optimization,'' in *Evolutionary Programming VII*, A. Eiben, V. Porto, N. Saravanan, and D. Waagen Eds. San Diego, California, USA: Springer-Verlag, 1998, pp. 591–600.

[26] C. Dong, G. Wang, and Z. Chen, ''The inertia weight self-adapting in PSO,'' in *Proc. 7th World Congr. Intell. Control Autom.*, 2008.

WEIBIN ZHU was born in Jiaozuo, China, in 1976. He received the B.E. degree in electronic engineering from the Changchun Institute of Optics and Fine Mechanics, Changchun, China, in 1998, and the Ph.D. degree in control theory and control engineering from Zhejiang University, Hangzhou, China, in 2014.

He joined China Jiliang University, in 2001, where he is an Associate Professor. His current interests include the grating signal processing and high-precision vision metrology.

YU LIN was born in Wenzhou, China, in 1995. She received the bachelor's degree from China Jiliang University, Hangzhou, China, in 2017, where she is currently pursuing the master's degree. Her research interest includes the grating signal processing and its applications.

YAO HUANG was born in Beijing, China, in 1982. He received the B.E. degree from the Beijing University of Technology, Beijing, China, in 2007. He is currently pursuing the Ph.D. degree with Zhejiang University, Hangzhou, China.

He has worded in the Geometric Lab, Beijing Metrology Institute, from 2007 to 2013. He joined the Division of Metrology in Length and Precision Engineering, National Institute of Metrology, in 2013.

ZI XUE, photograph and biography not available at the time of publication.